

Flow-Induced Platelet Activation in Bileaflet and Monoleaflet Mechanical Heart Valves

WEI YIN,¹ YARED ALEMU,¹ KLAUS AFFELD,² JOLYON JESTY,³ and DANNY BLUESTEIN¹

¹Department of Biomedical Engineering, State University of New York at Stony Brook, Stony Brook, NY 11974-8181;

²Biofluidmechanics Laboratory, Charite, Humboldt University of Berlin, 14050 Berlin, Germany; and ³Division of Hematology, Department of Medicine, Stony Brook University, Stony Brook, NY 11794

(Received 23 December 2003; accepted 1 April 2004)

Abstract—A study was conducted to measure *in vitro* the procoagulant properties of platelets induced by flow through Caromedics bileaflet and Bjork–Shiley monoleaflet mechanical heart valves (MHVs). Valves were mounted in a left ventricular assist device, and platelets were circulated through them under pulsatile flow. Platelet activation states (PAS) were measured during circulation using a modified prothrombinase method. Computational fluid dynamics (CFD) simulations of turbulent, transient, and non-Newtonian blood flow patterns generated by the two valve designs were done using the Wilcox $k - \omega$ turbulence model, and platelet shear-stress histories (the integral of shear-stress exposure with respect to time) through the two MHVs were calculated. PAS measurements indicated that the bileaflet MHV activated platelets at a rate more than twice that observed with the monoleaflet MHV. Turbulent flow patterns were evident in CFD simulations for both valves, and corroborated the PAS observations, showing that, for particles close to the leaflet(s), shear-stress exposure in the bileaflet MHV can be more than four times that in the monoleaflet valve.

Keywords—Thromboembolism, Blood flow, Computational fluid dynamics, Left ventricular assist device.

INTRODUCTION

Platelets and Shear Stresses

Platelets are ellipsoid discs 2–4 μm in diameter. They have important functions in both normal hemostasis and the pathologic clot formation seen in thrombosis. Among other causes, thrombosis may result from vascular stenosis caused by atherosclerosis, infection or trauma, or by abnormal blood flow around such abnormalities.¹⁰ Many research groups have used rheological methods to study the effects of shear stresses on platelets and it is well accepted that shear stress causes platelet activation.¹¹ Under abnormal flow conditions, shear-induced platelet activation can cause both aggregation (adhesion of platelets to each other in the

presence of fibrinogen) and—through provision of anionic phospholipid—thrombin generation. It is this latter reaction that we use to measure the activation state of platelets.

Mechanical Heart Valves (MHVs) and Thromboembolism

It is estimated that almost 2 million individuals have received prosthetic heart valves (PHVs), with approximately 120,000 valves implanted each year in the United States, of which about 60% are MHVs.⁶ The main complication of MHVs is thromboembolism, resulting especially in ischemic attacks and stroke. Recent studies conducted in animals³⁰ and patients^{9,17} strongly indicate that platelet activation is a major underlying mechanism in thromboembolism. It was reported recently (REMATCH study)²⁹ that Left Ventricular Assist Devices (LVAD) are superior to drug therapy, paving the way for their ultimate use—a long-term heart replacement therapy for patients not eligible for heart transplants. However, if approved for destination therapy, LVAD has only a 30% 2-year survival and an unacceptable complication rate of thrombosis/stroke. It is highly likely that most pathologic clot formation is a result of platelet activation caused by nonphysiological flow patterns induced by MHV.⁴ Even when correctly aligned,²⁷ MHVs may induce jet flow, elevated shear stresses, areas of flow separation and recirculation, shed vortices, and turbulence. Any of these factors may induce platelet activation and lead to formation of platelet plugs and clots. Even though new valve designs have reduced thromboembolic complication rates, the incidence of thromboembolism can still reach 1.5–3 per 100 patient years.⁷ These numbers may not be as high as rates of thromboembolism induced by other sources, such as atrial fibrillation,²⁰ but when considering the devastating consequences cardioembolic strokes may have on the patients with MHVs, these numbers are very significant. Thromboembolism is dependent on the type of the MHV implanted.²⁸ Laas *et al.*¹⁸ studied flow in the aortic root *in vivo* after mechanical aortic valve replacement (St. Jude Medical and Medtronic Hall) and observed that

Address correspondence to Danny Bluestein, PhD, Department of Biomedical Engineering, HSC T18-030, State University of New York at Stony Brook, Stony Brook, NY 11974-8181. Electronic mail: danny.bluestein@sunysb.edu

flow patterns through the aortic valve were asymmetric because of the angle between longitudinal axes of the left ventricle and the aortic root. Animal studies conducted by Kleine *et al.*¹⁶ demonstrated that tilting-disc monoleaflet MHVs (Medtronic Hall) provide optimum, almost physiologic flow, because they have a large orifice facing the area of major flow along the noncoronary leaflet. In comparison, the St. Jude Medical bileaflet MHV, which is most commonly used in heart valve replacement, could not generate a similar hemodynamic performance even at its optimal orientation. The leaflet geometry of the CarboMedics bileaflet MHVs (CM) is very similar to that of the St. Jude Medical bileaflet MHVs. Recent comparative nonrandomized studies demonstrated that there are no significant differences between the two in number of thromboembolic events, nonstructural dysfunction, and other valve-related complications.^{13,21} Lund *et al.*²⁴ reported that the mortality rate of St. Jude Medical bileaflet MHV 10 years after valve replacement was $42 \pm 5\%$; Lindblom *et al.*²² reported a mortality of 30% for Bjork–Shiley MHV; and Butchart *et al.*⁵ reported 36% for the Medtronic Hall MHV. Besides valve design, other factors such as age, sex, ethnicity, and degree of maintenance of adequate anticoagulation regimen can affect the mortality after MHV implantation.

Laas *et al.*¹⁹ also studied the high-intensity transient signal caused by free emboli after St. Jude Medical MHV implantation and demonstrated that the combination of valve tilt and insertion of subannular pledgets led to a significant increase in the thromboembolic potential of the valve, likely caused in part by increased platelet activation.

In this study, we have conducted experiments *in vitro* to quantify the platelet activation induced by flow through monoleaflet (Bjork–Shiley) and bileaflet (CarboMedics) MHVs mounted in an LVAD. In parallel, computational fluid dynamic (CFD) simulations were done in a physiological geometry to predict flow patterns in such MHVs that may induce platelet activation by these valves *in vivo*.

MATERIALS AND METHODS

Platelets

Outdated (80 h) apheresis units of platelets were obtained from Stony Brook University Hospital blood bank or from Long Island Blood Services (Melville, NY). One hundred milliliters was gel-filtered through a 1000-ml column of coarse Biogel A50M (2.7% agarose beads; Biorad, Hercules, CA) at a flow rate of 13 ml/min. Agarose beads were equilibrated in platelet buffer, which is a Hepes-modified Ca^{2+} -free Tyrodes buffer.²⁶ The gel-filtered platelet pool was counted (Z1 particle counter; Coulter, Hialeah, FL) and adjusted with platelet buffer to a concentration of $100,000 \mu\text{l}^{-1}$. Platelets were maintained at room temperature on a gentle shaker and used within 6 h after gel filtration.

Platelet Activation State (PAS) Assay and Statistics

PAS of timed samples from the circulation loop were measured by the prothrombinase method of Jesty and Bluestein¹⁴ as modified by Jesty *et al.*¹⁵ The base PAS activities of outdated pheresis platelets varied from 1 to 7% of the maximum. To establish a positive control and a reference maximum PAS value, a sample was removed at the end of each circulation experiment and fully activated by the addition of 1/40 volume 0.2 mM calcium ionophore A23187 in dimethylsulfoxide, followed by a 3-min incubation. PAS values presented here were normalized to the activity of this ionophore-activated sample, and are presented as normalized ratios. For each circulation experiment, the plot of normalized PAS vs. time was fitted by linear regression to obtain a platelet activation rate. Since the normalized PAS values are dimensionless, the dimension of platelet activation rate is time^{-1} . Mean platelet activation rates under the different valve conditions were compared using Student's paired *t* test. The data was further analyzed using the Wilcoxon signed-rank test to further confirm the paired *t* test results without assuming normal distribution (as is assumed in a paired *t* test). For this nonparametric analysis, the differences were ranked by their magnitude and then assigned the sign of the differences and summed to obtain the test statistic *W*.

Individual gel-filtered platelet preparations, usable for only 6 h, vary in both their base activation state and their sensitivity to activation. Platelets also slowly activate with storage. Each day's experiments, using one platelet preparation, were performed under two conditions (monoleaflet MHVs vs. bileaflet MHVs), each being repeated twice. In each day's experimental set, the two conditions were performed in palindromic order to minimize artifacts caused by time-dependent changes in platelets, i.e., for monoleaflet (M) and bileaflet (B), the order was M-B-B-M or B-M-M-B.

Recirculation Studies of Platelets

Platelet activation measurements were performed in a circulation loop based on an LVAD, which is the implantable part of a pneumatic heart-assist system. The LVAD chamber has a 65-ml stroke volume and a total volume of about 100 ml (Fig. 1). Two MHVs, mounted in LVAD in opposition, control the direction of circulation, the output and input being connected by a compliance reservoir (Fig. 2) made of 5-in. clinical grade surgical Penrose tubing (Bard Inc., Covington, GA). The LVAD diaphragm was driven in a pulsatile cycle by an external reciprocating pump (Harvard Apparatus model 1423) capable of producing quasi-physiological flow curves and regulation of both stroke volume and stroke rate (Fig. 2). To ensure minimal compliance and accurate definition of the pulsatile characteristics, water, rather than air, was used to drive LVAD. The pump rate was fixed at 4.7 l/min with

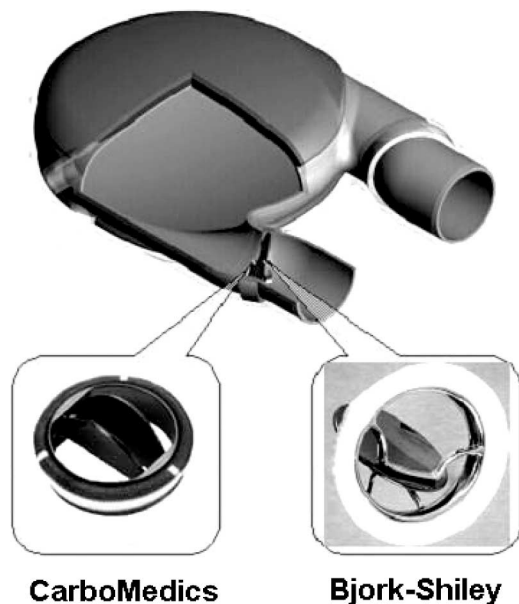


FIGURE 1. The left ventricular assist device (LVAD), with Bjork-Shiley monoleaflet and CarboMedics bileaflet MHVs.

a stroke rate of 72 min^{-1} and a systolic/diastolic ratio of 0.375, representing a normal cardiac output. The lifetime of platelets in the normal circulation is about 7 days, and on average a platelet passage through the left ventricle occurs every 90 s, corresponding to 6700 valve passages during the average platelet lifetime. The time chosen for the recirculation experiments was 30 min, corresponding (for two valve passages per LVAD cycle) to 2800 passages. Circulation experiments were done in an incubator at

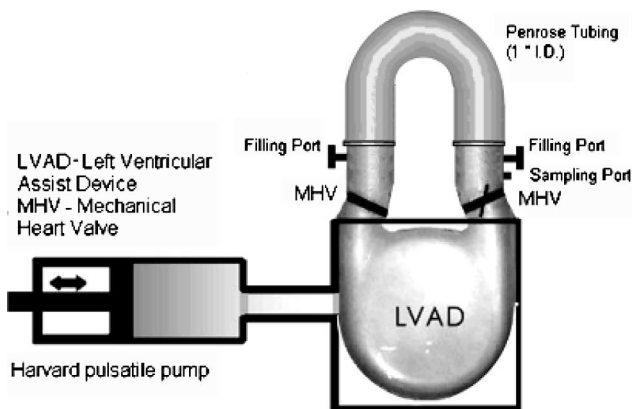


FIGURE 2. Schematic of the LVAD circulation loop. On the pump's drive stroke the water compresses the LVAD diaphragm, forcing the platelet suspension through the output valve into the compliance reservoir, the opposed valve remaining closed. On the return pump stroke, the diaphragm is under negative pressure, drawing the platelet suspension from the reservoir through the opposing input valve into the LVAD body. Each stroke is about 65 ml, with a stroke rate of about 70 ml/min.

$37 \pm 2^\circ\text{C}$. Timed aliquots were removed from the loop every 5 min and assayed immediately for PAS activity.

To account for platelet activation by LVAD itself, control experiments were conducted with MHVs removed. Without the valves controlling the flow direction, the platelet suspension passed back and forth between LVAD and the compliance reservoir.

Computational Fluid Dynamics

Turbulent/transient 2-D simulations of non-Newtonian flow through a CarboMedics bileaflet MHV and a Bjork-Shiley monoleaflet MHV in an anatomically correct aortic implantation position were conducted, to study the flow dynamics and to compare platelet shear histories for each valve. Because valves are often implanted *in vivo* in nonoptimal orientation, simulations for both valves were performed with the valve orientation 15° off the flow axis. The unsteady Reynolds-averaged Navier-Stokes equations were solved using Wilcox's $k - \omega$ model,³³ which is primary intended for simulating globally low- Re internal flows, with intermittent turbulent flows in the transitional range. Unlike the traditional $k - \epsilon$ turbulence model, which assumes an isotropic turbulence through the flow cycle ($Re > 10,000$), the $k - \omega$ model is able to account for sudden changes in main-strain rate and predict the variation of turbulence variables through the viscous sublayer all the way to the wall.

The calculation was performed for the first 300 ms following peak systole, during the deceleration phase, until just before the start of leaflet closure. Valve leaflets are therefore assumed to remain fully open. This phase in the flow cycle was chosen because during deceleration a turbulent jet develops through the valve orifices, followed by a wake of shed vortices, which entrain and activate platelets, and perhaps contribute to the formation of free emboli.^{1,2}

At low shear rates, such as occur in the recirculation zones and the shed vortices in the valve's wake, the non-Newtonian properties of blood may overwhelm its Newtonian properties. Accordingly, the blood was modeled as a non-Newtonian viscoelastic fluid with a density of 1.2 g/ml and a yield shear of 0.1 s^{-1} .²⁵ (It should be noted that this condition deliberately mimics the properties of blood, rather than the aqueous medium used in the experimental platelet study. In particular, the viscosity of whole blood is approximately 3.5 times that of saline buffer.)

The FIDAP CFD package (Fluent Inc., Lebanon, NH) was used for numerical simulations, and the numerical mesh was generated with the GAMBIT package (Fluent Inc.). The temporal value of the velocity applied at the inlet was taken from a typical physiological waveform.² It was allowed to evolve from a uniform flow at the inlet to a fully developed turbulent profile through a straight section of length 10 diameters, then allowed to accelerate through the converging section, e.g., from the 300 mm/s peak value to approximately 900 mm/s at the valve's annulus ($D = 81 \text{ mm}$ on

the ventricular side and $D = 27$ mm on the aortic side). Similarly, 12 diameters exit length were used to eliminate outlet effects. A physiological pressure gradient was simulated at the inlet and zero stress at the outlet, after establishing that the flow was fully developed by running a steady flow simulation.

A structured mesh was used throughout the flow domain except in the vicinity of the valve. A progressive density mesh, as required by the $k - \omega$ turbulent model, was used with sufficient resolution to capture the boundary layer flow near the solid edges and was also employed at the inlet of the flow domain. After establishing the numerical results to be independent of mesh density in all directions, the 2-D mesh consisted of 89,000 computational nodes and 23,000 elements. Approximately 290 time steps were required for convergence of the transient solution.

To quantify the shear-stress histories of the platelets, individual trajectories of platelets close to the valve leaflet(s) were calculated using the Lagrangian approach of particulate two-phase flow. A stochastic model that simulates the action of turbulence on the platelets was used for computing the trajectories.^{2,8} The values of viscosity, turbulent viscosity, kinetic energy, dissipation, and strain rate were extracted from the numerical solution and used to compute the platelet stress histories along the trajectories. Briefly, the cumulative effect of shear stress (τ) and exposure time (Δt) was computed by summation of the product of their instantaneous absolute values in each computational node along the platelet path, i.e., $\Sigma(\tau \times \Delta t)$.¹ The total stress, laminar plus turbulent, was computed using the Boussinesq approximation¹² and multiplied by the instantaneous exposure time to this stress (Δt_i), according to the following formulation:

$$\sum_{i=t_0}^{t_{\max}} \left(\frac{(\varepsilon_i + \varepsilon_{i+1})}{2} \times (\mu_i + \rho \mu_i^t) + KE_i \times \rho \right) \times \Delta t_i \quad (1)$$

where ε_i is the strain, μ_i is the viscosity, μ_i^t is the turbulent viscosity, ρ is the density, KE_i is the turbulent kinetic energy, and Δt is the time step.

RESULTS

Experimental

A comparison of platelet activation during circulation through a CarboMedics bileaflet MHV and a Bjork–Shiley monoleaflet MHV is shown in Fig. 3. In both cases, PAS values were normalized with reference to the maximum platelet activation determined after the experiment by ionophore activation (see Methods). The rate of activation by the bileaflet MHVs was $8.11 \times 10^{-4} \text{ min}^{-1}$, and with the monoleaflet MHVs was $3.14 \times 10^{-4} \text{ min}^{-1}$. Analysis of the collected activation rates for the two conditions by Student's t test showed the difference to be significant ($P < 0.05$), and a nonparametric sign test (Wilcoxon signed-rank test) of the

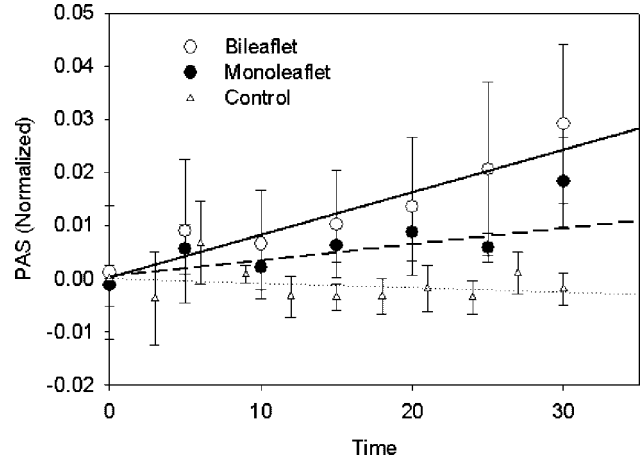


FIGURE 3. The PAS activities of platelets during circulation in LVAD. Platelets, at the concentration of $100,000/\mu\text{l}$ in buffer, were circulated at $37 \pm 2^\circ\text{C}$ and samples were removed for the measurements every 5 min. It shows PAS \pm SEM, normalized to the activity of ionophore-activated suspension. The mean zero-time intercept for each set was subtracted to enable visual comparison. Individual runs were fitted by linear regression to obtain individual rates of platelet activation. The lines shown in the figure were the mean slopes of the collected experimental runs. Bileaflet MHV (slope = $8.114 \times 10^{-4}/\text{min}$) generated higher PAS activities than the monoleaflet MHV (slope = $3.143 \times 10^{-4}/\text{min}$). The difference between the two was significant ($P < 0.05$). The control line (slope = 8.5×10^{-5}) demonstrated there was no significant activation in the control loop at the end of 30 min, indicating that the flow through MHVs, rather than contact activation, was the main source of the platelet activation.

daily sets of paired data, based on the computed W value, gave $P < 0.03$. Figure 3 also shows the lack of platelet activation in the absence of valves, confirming that the activation observed is dependent on the valves themselves.

CFD Simulations

A parallel CFD study was done to compare bileaflet and monoleaflet MHVs in order to study whether the difference in valve-dependent platelet activation that were measured in the experimental circulation system correspond to differences in shear-stress history that are predicted by a computational approach, simulating conditions that pertain for implanted valves *in vivo*. For both valves, the valve axis was set at 15° off the major blood flow axis to reflect the common surgical situation of misalignment during implantation. The simulated misalignment is similar, but not identical, to the mounting of the experimental valves in LVAD, where the valve is also misaligned in respect to the major flow axis.

The computed velocity vector field through a bileaflet MHV at 198 ms after peak systole is depicted in Fig. 4. A flow separation followed by a wake of shed vortices effectively decreased the orifice area between the valve leaflets, producing strong turbulent jet flow. The highest flow velocity at this phase was 134 cm/s. The transient simulation

indicated that as the flow velocity decreased, the shed vortices lost energy and eventually subsided, just before the leaflets' closure phase (approximately 300 ms into the deceleration phase).

Owing to their different geometric and dynamic properties, the flow patterns developed through the monoleaflet MHV were very different from those through the bileaflet MHV. The transient simulation indicated a faster deceleration of the blood flow and earlier appearance of shed vortices for the monoleaflet MHV. At about 198 ms after peak systole the shed vortices in the wake of the monoleaflet MHV had lost most of their energy and subsided, while at the same time point the bileaflet MHV wake of shed vortices was still very potent. Thus, comparing the two valves at the same time points would be inadequate. As similar flow patterns with shed vortices through the monoleaflet MHV occur at a much earlier phase—20 ms after peak systole (Fig. 5)—this time point was selected as representing flow dynamics comparable to those of the bileaflet MHV at 198 ms. Owing to the unique geometry of the Bjork–Shiley monoleaflet MHV, vortices develop around the leaflet itself. Two or three vortices were shed behind the leaflet and quickly subsided, generating a much shorter wake. Because the single leaflet in this valve is quite well aligned with the major blood flow axis, the flow through the major and minor orifices of the valve was minimally affected. The highest flow recorded was 167 cm/s, significantly higher than seen with bileaflet MHV. However, the transient simulation indicated a much faster velocity drop in the monoleaflet MHV after peak systole.

In vivo, the shear layers formed in the interface between the jet flow and recirculation zones can produce elevated shear stresses, which we predict contribute to platelet activation. Activated platelets trapped in the recirculation zones will be potentially entrapped within the shed vortices, where optimal conditions exist for forming aggregates and leading to thromboembolus formation. To study the elevated shear stresses in these shear layers in our simulation, platelet-simulating particles were seeded slightly upstream of the valves' leaflets. Their shear-stress histories (total stress accumulation, which will mimic platelet activation) were computed along such pertinent trajectories, using the stochastic algorithm described in Methods. For each valve, numerous trajectories were computed in the region of highest shear stresses near the leaflets, and in the low shear-stress core flow region, which was used as a reference shear-stress history for each valve. The computation was performed during deceleration, corresponding to the phase during the cardiac cycle when vortices were shed and turbulence peaked. Typical particle trajectories are depicted in Fig. 6. They are representative samples of particle trajectories. Repeated computations indicated that, for both valve types, particles close to valve leaflet tended to get trapped within the shed vortices of the wake. The level of shear stresses close to the leaflets was much higher than in the core

flow region. The maximum particle shear-stress history in a typical trajectory close to the leaflet of the bileaflet MHV ($20 \text{ dyne s cm}^{-2}$) was markedly higher than that in a similar trajectory in the monoleaflet MHV (5 dyne s cm^{-2}). Additionally, however, the bileaflet MHV accumulated shear stresses faster in the core flow as, as compared to the corresponding regions of the monoleaflet MHV, and this may constitute a significant part of the overall bulk exposure of particles to shear stress in passage through MHVs.

DISCUSSION

As we noted in the Introduction to this paper, many pieces of evidence over several years have strongly suggested that much of the increased risk of thromboembolism in patients with implanted MHVs is probably caused by the valves' activating platelets. The experimental evidence reported here, of studies of isolated platelets in a well-controlled circulation system *in vitro*, not only directly confirms such activation, but also demonstrates clearly that the extent of platelet activation is dependent on the valve type. However, although the ability to measure platelet activation caused by their passage through MHVs is a significant advance, it does not address the detailed question of when or where platelet activation occurs, or what aspect of valve design is critical in this activation. For that we turned to computational simulation, and a study of the stress history of particles in flow fields through valves, using initial conditions that mimic those of an implanted valve *in vivo*.

In the experiments in the circulation system described, it is impossible to determine the platelet shear-stress history. In particular, just as is true of implanted mechanical heart valves *in vivo*, only a fraction of the platelets that pass through the valve are exposed to elevated shear stresses. Thus, platelets sampled from the circulation loop are a sample of the bulk population, with varying shear-stress histories. Given the limited exposure of platelets to shear in the valves, the ability to distinguish between the shear-stress histories induced by the monoleaflet and bileaflet valves is quite striking; and it serves to demonstrate the value of the PAS assay in measuring small activation levels induced by MHVs or similar devices. We have demonstrated¹⁵ not only that the assay can measure low levels of platelet activation, but also that it has the benefit of being a near-real-time measurement suitable for time-resolved studies of multiple samples.

Nonetheless, LVAD-based circulation system is subject to a number of constraints that make parallels with the situation *in vivo* inexact. Neither whole blood nor platelet-rich plasma can be used, since the PAS assay is optically based, and additionally requires that normal prothrombin be absent. Second, because of the large volumes required, freshly drawn platelets cannot be used. Outdated pheresis platelets, although adequate to the task, are commonly partially activated, not only because they are outdated but probably also

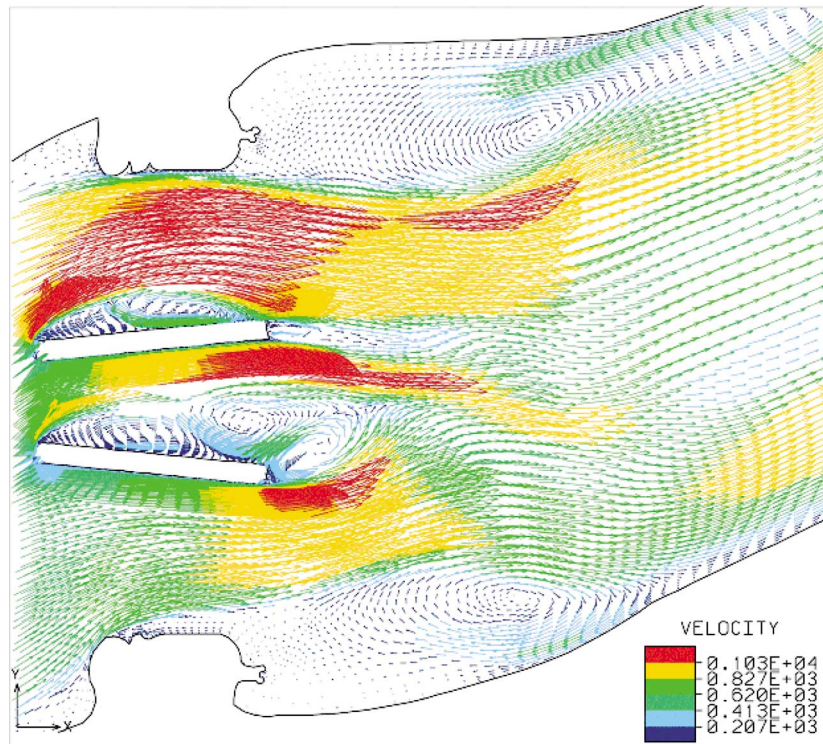


FIGURE 4. CFD simulation of the bileaflet MHV in the aortic position at 198 ms after peak systole. Shedding vortices developed in the valve area. A wake with shed vortices was generated between the leaflets, which effectively decreased the orifice area between the valve leaflets and narrowed the blood flow passages, producing strong jet flow. The highest flow velocity was 134 cm/s.

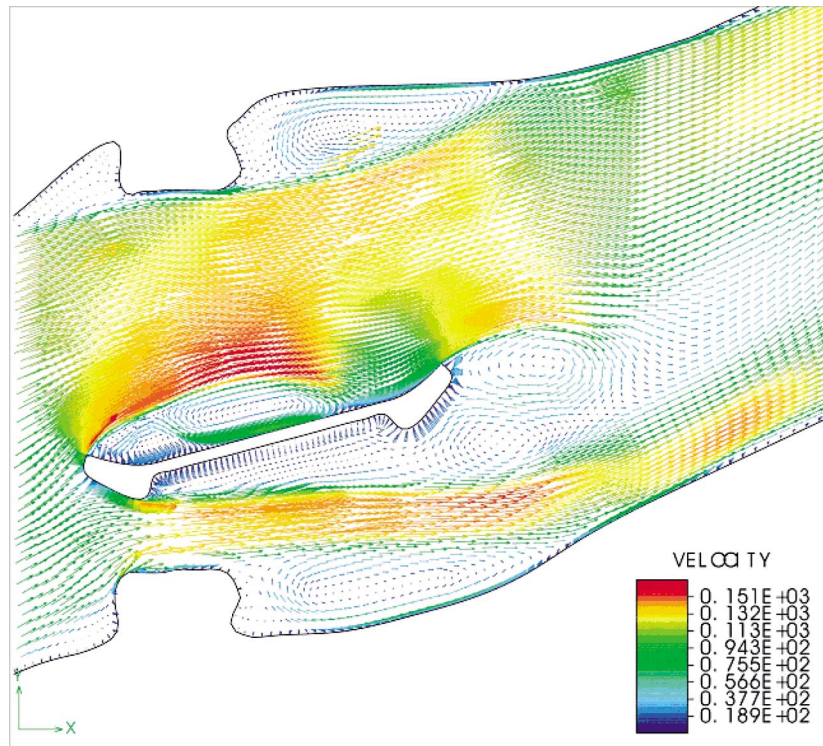


FIGURE 5. CFD simulation of the monoleaflet MHV in the aortic position at 20 ms after peak systole. The valve was tilted, resulting in an alignment between the valve leaflet and the major blood flow. A big wake formed immediately after the valve. The highest flow velocity was 167 cm/s.

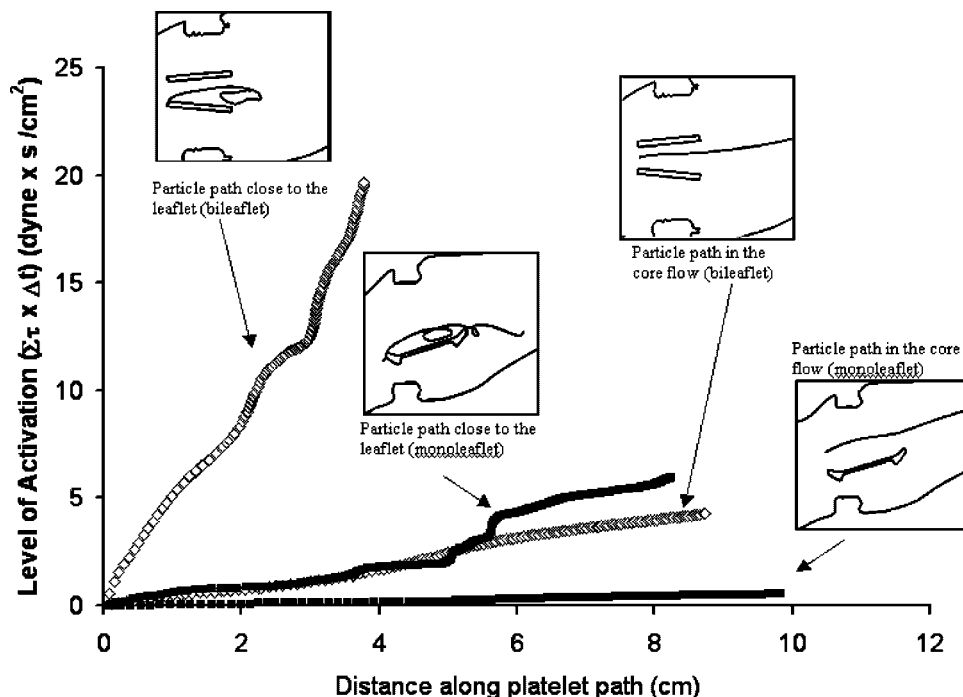


FIGURE 6. Comparison of shear-stress histories of platelets (level of activation) along the platelet path in the core flow and near the valve leaflet for the bileaflet MHV and monoleaflet MHV. Platelets were activated faster in bileaflet than in monoleaflet both in core flow and near the valve leaflet.

because pheresis machines themselves likely cause some degree of platelet activation. The range of base PAS in such platelets is wide, in our experience varying from 1 to 7% of their maximum attainable activity. In contrast, freshly prepared platelets range from 0.5 to 2.5%. The third constraint arises from the use of plasma free platelets. This, however, is also an advantage, in that the lack of von Willebrand factor reduces the likelihood of surface adhesion and adhesion-dependent activation and, similarly, the lack of fibrinogen prevents platelet aggregation. Thus the method allows us to focus primarily on activation caused, or at least initiated, by mechanical stress. That this is so is confirmed by the controls in which valves were removed from LVAD. Without valves, the platelets do not circulate, but they do flow back and forth between LVAD and the compliance reservoir with each pulse (Fig. 2). Under these conditions the observed mean platelet activation rate was essentially zero (Fig. 3). Another constraint is that the small circulation system does not provide a proper afterload or backpressure on the valves. Resistance devices cannot be used in the circulation loop, since they would produce unacceptable levels of shear stress. Nonetheless, we emphasize that, despite these constraints, the flow system used here duplicates much of the essential parameters of flow through MHVs.

Unlike circulation studies, numerical simulation can predict particle shear-stress histories along computed trajectories at any position in the flow field. The physiological geometry of the left ventricle and the aorta was used in

the numerical simulation, to simulate blood flow patterns *in vivo* after valve implantation, and to verify whether the differences in platelet activity measured in the circulation system *in vitro* pertain to the implantation conditions *in vivo*. In this study, a 2-D instead of a 3-D model was used. In case of turbulence, a 2-D model may slightly distort the vector field and tend to elongate shed vortices in the major flow direction, but can still provide a fairly accurate quantitative depiction of the flow field after MHV implantation. In a previous study³ a good correlation was established between 2-D turbulent simulations and detailed DPIV measurements in a wake of a St. Jude Medical MHV.

Because of the differences between the monoleaflet MHV and the bileaflet MHV, shed vortices do not appear at the same times after peak systole. Accordingly (as detailed in the Results section) particle shear-stress histories were computed at different time points (198 ms after peak systole for the bileaflet MHV, and 20 ms after peak systole for the monoleaflet MHV). We observed that the large flow separation zone formed above the bileaflet MHV leaflets effectively narrowed the blood flow passage area, resulting in stronger jets through the valve orifices, stronger wakes, and more shed vortices as compared with the monoleaflet MHV (Figs. 4 and 5).

Kolmogorov length scales³² could be used to roughly estimate the length scales of the smallest turbulent eddies, the turbulent structures which may dissipate energy on the blood cells. When the Kolmogorov scales are comparable

to cellular diameters, the turbulent shear stresses can activate or disrupt blood cells. According to our CFD computation, the smallest eddy size is $\eta_k \approx (V^3/\varepsilon)^{1/4} = 4.66 \mu\text{m}$, which is very close to that of platelets ($4 \mu\text{m}$). This Kolmogorov scale of turbulent eddies in blood flow past MHV poses a direct threat to the platelets²³ resulting in a much higher strain energy dissipated on platelet membranes, making them more prone to shear-stress activation.³¹

The high shear stresses induced by MHVs are very favorable for rapid platelet activation. For the monoleaflet valve the flow passage area available was much larger, and its better alignment with the major axis of flow prevented the formation of such a large flow separation above the leaflet. The wake was formed in close vicinity to the leaflet's trailing edge, and was much shorter, resulting in less exposure to areas of high shear stress.

Valve misalignment during MHV implantation, which is difficult to control in surgery but often occurs, can generate narrower and stronger jet flow through the valve orifices and a wide wake with shed vortices, especially in bileaflet MHVs. For this reason we incorporated a mild (15°) misalignment in setting up the computational study. Under these conditions particles close to the valve leaflet are exposed to high shear stresses and can eventually get trapped within the shed vortices of the wake, as shown by the trajectories in Fig. 6. The shear-stress history of particles near the leaflet of the bileaflet MHV indicated a rapid increase in shear stress, reaching a value of $20 \text{ dyne s cm}^{-2}$ over a short span during just a single passage (distance along the trajectory of 4 cm). For the monoleaflet MHV, particles close to the valve leaflet attained a shear-stress history of about 5 dyne s cm^{-2} over a longer trajectory of 8 cm.

Although shear stresses in the core region of MHVs are much lower, the differences remain, with the bileaflet MHV generating shear-stress histories about fivefold higher than the monoleaflet MHV. Besides elevated shear stresses, the particles were also exposed to deformation stresses due to the acceleration in jets, followed by the rapid deceleration in the wake. Under the combination of shear and deformation stresses *in vivo*, platelets tend to get activated more rapidly.² Furthermore, turbulence increases the collision frequency and contact between potentially activated platelets, potentially enhancing the formation of platelet aggregates.

The computational simulation was performed with the leaflets in the fully open position, without considering the contribution of other cardiac cycle flow phases, e.g., regurgitant flow during diastole, leaflet closure, effects of flow in the valve hinge regions, and the flow dynamics (all of which the platelets were subjected to in the experimental part of this study). However, it is during the flow deceleration following peak systole that the wake of shed vortices starts to appear, which would provide potentially activated platelets the needed flow conditions to form aggregates which would become the source of thromboemboli. As the valves close, the shed vortices subside and the wake is destroyed. Our

simulations clearly demonstrate that because of the unique combination of elevated stresses and longer residence times, it is the stress accumulation during this flow phase that is so rapid. We hypothesize that these shed vortices, and the ensuing exposure to shear stress, are the origin of cerebrovascular microemboli associated with MHVs, and we are currently studying a sheep model to test this hypothesis *in vivo*.

Recognizing the overlooked flow induced mechanisms leading to thromboembolism in MHV and other blood circulating devices can help to improve their design. The methodology described here within will facilitate better device design. It may reduce the risks for the patients who have these devices implanted, lower the ensuing healthcare costs and offer viable long-term solutions for the patients.

ACKNOWLEDGMENT

This work was supported in part an Established Investigator Award from the American Heart Association (DB) and by the National Science Foundation under Grant No. 0302275 (DB).

REFERENCES

- ¹Bluestein, D., Y. M. Li, and I. B. Krukenkamp. Free emboli formation in the wake of bi-leaflet mechanical heart valves and the effects of implantation techniques. *J. Biomech.* 35:1533–1540, 2002.
- ²Bluestein, D., C. L. Niu, R. T. Schoepfoerster, and M. K. Dewanjee. Fluid mechanics of flow through a stenosis: Relationship to the development of mural thrombus. *Ann. Biomed. Eng.* 25(2):344–356, 1997.
- ³Bluestein, D., E. Rambod, and M. Gharib. Vortex shedding as a mechanism for free emboli formation in mechanical heart valves. *J. Biomed. Eng.* 122(2):125–134, 2000.
- ⁴Bluestein, D., W. Yin, K. Affeld, and J. Jesty. Flow-induced platelet activation in mechanical heart valves. *JHVD* 13:501–508, 2004.
- ⁵Butchart, E. G., H. H. Li, N. Payne, K. Buchan, and G. L. Grunkemeier. Twenty years experience with the Medtronic Hall valve. *J. Thorac. Cardiovas. Surg.* 121:1090–1100, 2001.
- ⁶Cary, W., and M. D. Akins. Results with mechanical cardiac valvular prostheses. *Ann. Thorac. Surg.* 60:1836–1844, 1995.
- ⁷Edmunds, L. H., Jr., S. Mckinlay, J. M. Anderson, T. H. Callahan, J. H. Chesebro, E. A. Geiser, D. M. Makanani, L. V. McIntire, W. Q. Meeker, G. N. Naughton, J. A. Panza, F. J. Schoen, and P. Didisheim. Directions for improvement of substitute heart valves: National heart, lung and blood institute's working group report on heart valves. *J. Biomed. Mater. Res.* 38(3):263–266, 1997.
- ⁸Gosman, A. D., and E. Ioannides. Aspects of computer simulation of liquid-fuelled combustors. *AIAA J. Energy* 7(6):482–490, 1983.
- ⁹Gresele, P., and G. Agnelli. Novel approaches to the treatment of thrombosis. *Trends Pharmacol. Sci.* 23(1):25–32, 2002.
- ¹⁰Guyton, A. C., and J. E. Hall. *Text Book of Medical Physiology*. Philadelphia: W. B. Saunders, 1996, 463 pp.
- ¹¹Hellums, J. D. Biorheology in thrombosis research. *Ann. Biomed. Eng.* 22:445–455, 1994.

- ¹²Hinze, J. O. *Turbulence*. New York: McGraw-Hill, New York, 1987, pp. 22–23, 493.
- ¹³Jamieson, W. R., R. T. Miyagishima, G. L. Grunkemeier L. H. Burr, S. V. Lichtenstein, and E. F. O. Tyers. Multiple mechanical valve replacement surgery comparison of St. Jude Medical and CarboMedics prostheses. *Eur. J. Cardiothorac. Surg.* 13:151–159, 1998.
- ¹⁴Jesty, J., and D. Bluestein. Acetylated prothrombin as a substrate in the measurement of the procoagulant activity of platelets: Elimination of the feedback activation of platelets by thrombin. *Ann. Biochem.* 272:64–70, 1999.
- ¹⁵Jesty, J., W. Yin, P. Perrotta, and D. Bluestein. Platelet activation in a circulating flow loop: Combined effects of shear stress and exposure time. *Platelets* 14:143–149, 2003.
- ¹⁶Kleine, P., M. Perthel, H. Nygaard, S. B. Hansen, P. K. Paulsen, C. Riis, and J. Laas. Medtronic Hall vs. St. Jude Medical mechanical aortic valve: Downstream turbulences with respect to rotation in pigs. *JHVD* 75(5):548–555, 1998.
- ¹⁷Koster, A., M. Loebe, R. Hansen, E. V. Potapov, G. P. Noon, H. Kuppe, and R. Hetzer. Alternations in coagulation after implantation of a pulsatile Novacor LVAD and the axial flow MicroMed Debakey LVAD. *Ann. Thorac. Surg.* 70:533–537, 2000.
- ¹⁸Laas, J., P. Kleine, M. J. Hasenkam, and H. Nygaard. Orientation of tilting disc and bileaflet aortic valve substitutes for optimal hemodynamics. *Ann. Thorac. Surg.* 68:1096–1099, 1999.
- ¹⁹Laas, J., S. Kseibi, M. Perthel, A. Klingbeil, L. El-Ayoubi, and A. Alken. Impact of high intensity transient signals on the choice of mechanical aortic valve substitutes. *Eur. J. Cardiothorac. Surg.* 23:93–96, 2003.
- ²⁰Lamassa, D. C. A., G. Pracucci, A. Basile, G. Trefoloni, P. Vanni, S. Sppolveri, M. C. Baruffi, G. Landini, A. Ghetti, C. D. Wolfe, and D. Inzitari. Characteristics, outcome, and care of stroke associated with atrial fibrillation in Europe: Data from a multicenter multinational hospital-based registry (the Europe community stroke project). *Stroke* 32:392–398, 2001.
- ²¹Lim, K. H., M. Caputo, R. Ascione, J. Wild, R. West, G. Angelini, and A. J. Bryan. Prospective randomized comparison of CarboMedics and St Jude Medical bileaflet mechanical heart valve prostheses: An interim report. *J. Thorac. Cardiovasc. Surg.* 123(1):21–32, 2002.
- ²²Lindblom, D. Long-term clinical results after aortic valve replacement with the Bjork–Shiley prosthesis. *J. Thorac. Cardiovasc. Surg.* 95:658–667, 1988.
- ²³Liu, J. S., P. C. Lu, and S. H. Chu. Turbulence characteristics downstream of bileaflet aortic valve prostheses. *J. Biomech. Eng.* 122(2):118–124, 2000.
- ²⁴Lund, O., S. L. Nieelson, H. Aridsen, L. B. Illkjaer, and H. K. Pilegard. Standard aortic St. Jude valve at 18 years: Performance profile and determinants of outcome. *Ann. Thorac. Surg.* 69:1459–1465, 2000.
- ²⁵Merrill, E. W., E. R. Gilliland, G. R. Cokelet, H. Shin, A. Britten, and R. E. Well. Rheology of human blood, near and at zero flow. *Biophys. J.* 3:199–213, 1963.
- ²⁶Neuenschwander, P., and J. Jesty. A comparison of phospholipid and platelets in the activation of factor VIII by thrombin and factor Xa, and in the activation of factor X. *Blood* 76:1761–1770, 1988.
- ²⁷Omoto, R., M. Matsumura, H. Asano, S. Kyo, S. Takamoto, Y. Yokote, and M. Wong. Doppler ultrasound examination of prosthetic function and ventricular blood flow after mitral valve replacement. *Herz* 11(6):346–350, 1986.
- ²⁸Rahimtoola, S. H. Choice of prosthetic heart valve for adult patients. *J. Am. Coll. Cardiol.* 41(6):893–904, 2003.
- ²⁹Rose, E. A., A. J. Moskowitz, M. Packer, J. A. Sollano, D. L. Williams, A. R. Tierney, D. F. Heitjan, P. Meier, D. D. Ascheim, R. G. Levitan, A. D. Weinberg, L. W. Stevenson, P. A. Shapiro, R. M. Lazar, J. T. Watson, D. J. Goldstein, and A. C. Gelijns. The REMATCH trial: Rationale, design, and end points. Randomized evaluation of mechanical assistance for the treatment of congestive heart failure. *Ann. Thorac. Surg.* 67(3):723–730, 1999.
- ³⁰Snyder, T. A., M. J. Watach, N. L. Kenneth, and W. R. Wagner. Platelet activation, aggregation, and life span in calves implanted with axial flow ventricular assist devices. *Ann. Thorac. Surg.* 73:1933–1938, 2002.
- ³¹Travis, B. R., H. L. Leo, P. A. Shah, D. H. Frakes, and A. P. Yoganathan. An analysis of turbulent shear stresses in leakage flow through a bileaflet mechanical prostheses. *J. Biomech. Eng.* 124:155–165, 2002.
- ³²Travis, B. R., U. M. Marzec, J. T. Ellis, P. Davoodi, T. Momin, S. R. Hanson, L. A. Harker, and A. P. Yoganathan. The sensitivity of indicators of thrombosis initiation to a bileaflet prosthesis leakage stimulus. *J. Heart Valve Dis.* 10(2):228–238, 2001.
- ³³Wilcox, D. C. Simulation of transition with a two-equation turbulence model. *AIAA J.* 32(2):247–255, 1994.